Thermodynamics of Poly(dimethylsiloxane)/Poly(ethylmethylsiloxane) (PDMS/PEMS) Blends in the Presence of High-Pressure CO_2

Teri A. Walker,[†] Coray M. Colina,[†] Keith E. Gubbins,[†] and Richard J. Spontak*[,†,‡]

Departments of Chemical Engineering and Materials Science & Engineering, North Carolina State University, Raleigh, North Carolina 27695

Received July 2, 2003; Revised Manuscript Received January 15, 2004

ABSTRACT: Processing polymer blends in the presence of high-pressure carbon dioxide (CO_2) affords numerous advantages over organic solvents and is becoming a commercially viable and environmentally responsible alternative in the development of new multicomponent materials. A prerequisite to such processing is a fundamental understanding of how high-pressure CO_2 influences the phase behavior of polymer blends. In this work, we use high-pressure spectrophotometry to measure the cloud point (T_{cp}) of poly(dimethylsiloxane)/poly(ethylmethylsiloxane) (PDMS/PEMS) blends as a function of CO_2 pressure (P) in the vapor phase. Results obtained here at different blend compositions indicate that values of T_{cp} for this upper critical solution temperature (UCST) blend (i) generally increase with increasing pressure and (ii) collapse onto a master curve of $\Delta T_{cp}(P)$ for pressures up to about 35 MPa. These data are analyzed by the Sanchez−Lacombe equation of state to ascertain the temperature dependence of an effective interaction parameter (χ) in terms of $A + B/T$, where A and B are both pressure-sensitive. We also compare our results with previously reported data to delineate the role of hydrostatic pressure on the phase behavior of these blends.

Introduction

Numerous independent studies[1−5] have explored the utility of high-pressure carbon dioxide (CO_2) in conjunction with novel or facilitated polymer synthesis and processing operations over the past couple of decades. In these studies, CO_2 has served in various capacities such as solvent, cosolvent, plasticizer, penetrant, and foaming agent. Practical considerations motivating the use of CO_2 in these capacities include the following: (i) it is generally environmentally benign compared to many common organic solvents; (ii) it has tunable solvent properties due to its high compressibility around the critical point; (iii) it possesses a low and easily accessible critical point of 304.13 K (31 °C) and 7.37 MPa; and (iv) it can be readily separated from polymer systems by simple depressurization rather than by energy-intensive thermal evaporation. Since many polymer systems of technological relevance consist of two or more components,[6] extension of CO_2-based processing to these systems necessarily requires a fundamental understanding of how CO_2, temperature, and pressure influence the ability of the system to form a desired morphology with specific thermal and mechanical properties. It is therefore necessary to know the effect of high-pressure CO_2 on the phase behavior of multicomponent polymer systems so that appropriate processing (or application) conditions can be wisely chosen. The purpose of the present work is to help elucidate the fundamental thermodynamic behavior of polymer blends in the presence of high-pressure CO_2.

Carbon dioxide constitutes a good plasticizing agent for many different polymers.[7,8] In this regard, it promotes substantial changes in polymer physical properties. As CO_2 penetrates a polymer, it induces an increase in free volume and chain mobility, which promotes reductions in glass transition temperature (T_g), crystallization temperature and viscosity.[7−9] Enhanced chain mobility can likewise induce substantial molecular reorganization, such as crystallization of frozen-in amorphous media.[10] The effect of CO_2 on polysiloxanes is particularly noteworthy, since this class of polymers is generally CO_2-philic. In fact, addition of CO_2 to poly(dimethylsiloxane) (PDMS) is accompanied by substantial swelling (by at least a factor of 2[8,11]) and viscosity reduction (by nearly 2 orders of magnitude[12]). The phase behavior of multicomponent polymer systems, either physical blends or block copolymers, composed of constituent species that exhibit different degrees of CO_2-philicity is therefore expected to be strongly influenced by the presence of high-pressure CO_2. Independent studies in this vein have demonstrated that CO_2 can either enhance or reduce the miscibility of such systems, depending on factors such as solvent screening effects, dissimilar volume changes, and hydrostatic pressure effects. For upper critical solution temperature (UCST) blends[13] and upper disorder−order temperature (UDOT) copolymers[14] consisting of polystyrene (PS) and polyisoprene (PI), (micro)phase separation is driven by endothermic mixing. Addition of CO_2 to such systems effectively screens unfavorable interactions, resulting in enhanced miscibility. Subjecting a lower critical solution temperature (LCST) blend composed of PS and poly(vinylmethyl ether) (PVME)[15,16] or a lower disorder−order temperature (LDOT) block copolymer containing PS and poly(*n*-butyl methacrylate) (PnBMA) sequences[15] to CO_2, on the other hand, yields pronounced reductions in miscibility. Phase separation at substantially reduced temperatures reflects disparate CO_2-induced chain swelling due to selective CO_2 sorption.

While studies of high-molecular-weight polymer systems are ultimately necessary to establish key process paradigms with high-pressure CO_2, insight into the

* To whom correspondence should be addressed (Rich_Spontak@ncsu.edu).
[†] Department of Chemical Engineering, North Carolina State University.
[‡] Department of Materials Science & Engineering, North Carolina State University.

10.1021/ma034920o CCC: $27.50
Published on Web 03/12/2004

Table 1. Pertinent Thermodynamic Data Available for PDMS/PEMS Blends

$\bar{M}_w$ (PDMS/PEMS)	polydispersity index range	w_{PDMS}	A	B	ref
80000−115000/ 4000−9000	1.18−1.42	0.1−0.9	−0.002	4.07	22
27000/33800	1.06−1.12	0.30	−0.00695	4.52	24
		0.54	−0.0029	3.22	24
		0.82	−0.01154	6.42	24
19100/14000	1.02−1.03	0.36−0.54	−0.00958[a]	6.00[a]	18
8000/84000	1.08−1.14	0.1−0.9	−0.00334	5.59	23

[a] Analysis conducted in this work.

effect of CO_2 on polymer thermodynamics can be gleaned from model systems that do not suffer from broad molecular weight distributions or high viscosities. For this purpose, we have elected to investigate blends of PDMS and poly(ethylmethylsiloxane) (PEMS), which exhibit UCST behavior. Because of the low T_g of these polymers (typically between −150 and −120 °C),[17] their blends are molten at relatively low temperatures, including ambient temperature and above. Several studies have reported on the phase[18−23] and critical[24−27] behavior of, as well as interdiffusion[28] in, PDMS/PEMS blends in the absence of CO_2, thereby providing a solid baseline from which to proceed. Various strategies[19,22,24] have been used in an attempt to discern interaction parameters for this blend, and a summary of these previous activities is provided in Table 1. This blend is unusual in that it exhibits a negative ΔV_{mix}, which results in enhanced miscibility upon hydrostatic pressurization.[20,21] The change in the UCST of blends with pressure (P) can be described by $(\Delta\text{UCST}/\Delta P)_\phi = (T\Delta V_{mix}/\Delta H_{mix})$, where ΔH_{mix} is the heat of mixing and T denotes absolute temperature. Since ΔH_{mix} is positive (endothermic mixing) for UCST systems, the direction of the UCST shift is dependent on the sign of ΔV_{mix}.[29]

An earlier study[13] of PS/PI blends has revealed that hydrostatic pressure affects the phase behavior of this UCST blend differently than high-pressure CO_2. An increase in hydrostatic pressure promotes reduced blend miscibility, which is consistent with a positive ΔH_{mix} and a positive ΔV_{mix}. Exposure to high-pressure CO_2, however, results in initial miscibility enhancement, followed by a gradual reduction in miscibility at pressures higher than ∼20 MPa, depending on blend composition. These observations have been explained in terms of the competing effects between CO_2 plasticization (enhanced miscibility) and hydrostatic pressure (reduced miscibility). This competition can be understood qualitatively by recognizing that CO_2 molecules screen repulsive interactions, allowing dissimilar chains to intermingle more freely, while hydrostatic pressure squeezes the molecules together, forcing unfavorable contacts that induce phase demixing. On the basis of a lattice fluid model,[30] Beiner et al.[20] explain how a negative ΔV_{mix} could arise for blends such as PDMS/PEMS that have a small positive interaction parameter. According to this model, $\Delta V_{mix} = \phi(1-\phi)\{4\chi - [(\epsilon_{11} - \epsilon_{22})/RT]^2\}$, where ϕ represents the volume fraction of either constituent polymer, χ is the Flory−Huggins interaction parameter, ϵ_{ii} (i = 1 or 2) is the interaction energy between like species, and R is the universal gas constant. Thus, if the parameter χ is sufficiently small, the squared interaction energy term will dominate and ΔV_{mix} will be negative. A negative ΔV_{mix} is responsible for the enhanced miscibility achieved[20] in PDMS/PEMS blends upon hydrostatic pressurization. Since high-pressure CO_2 will swell the constituents of this blend, as well as shield their intermolecular interactions, we anticipate a priori that this system will be affected very differently by high-pressure CO_2 than by pure hydrostatic pressure. The present work examines the phase behavior of the PDMS/PEMS blend in the presence of CO_2, and predicts the dependence of an effective interaction parameter on pressure according to the Sanchez−Lacombe (S−L) equation of state.

Theoretical Background

The Flory−Huggins (F−H) equation of state is based on the concept of a lattice model and embodies the essential physical characteristics needed to distinguish mixtures composed of macromolecules from those containing only small molecules.[31] For a binary polymer blend, the F−H equation of state can be written as

$$\frac{\Delta G_{mix}}{kT} = \frac{\phi \ln \phi}{v_1 N_1} + \frac{(1-\phi)\ln(1-\phi)}{v_2 N_2} + \frac{\chi\phi(1-\phi)}{v} \quad (1)$$

where ΔG_{mix} is the free energy change upon mixing, k is the Boltzmann constant, v_i is the repeat unit volume of polymer i, N_i is the number of repeat units in polymer i, and v is a reference volume (either tabulated with values of v_i or computed as the geometric mean of the individual v_i). The thermodynamic conditions associated with the binodal (coexistence) curve of the phase diagram for a mixture require that

$$\mu_i(T,P,\phi_i^{I}) = \mu_i(T,P,\phi_i^{II}) = ... = \mu_i(T,P,\phi_i^{n}) \quad (2)$$

where μ_i is the chemical potential of component i in the mixture and the superscripts I, II, ..., n represent the different phases in equilibrium. Determination of μ_i from eq 1, coupled with the requirement of eq 2, yields the following closed-form analytical expressions for the coexistence curve of a binary polymer blend:[32]

$$\ln\left(\frac{\phi^{I}}{\phi^{II}}\right) + (\phi^{II} - \phi^{I})\left(1 - \frac{v_1 N_1}{v_2 N_2}\right) + \frac{\chi v_1 N_1}{v}((1-\phi^{I})^2 - (1-\phi^{II})^2) = 0 \quad (3a)$$

$$\ln\left(\frac{(1-\phi^{I})}{(1-\phi^{II})}\right) + (\phi^{I} - \phi^{II})\left(1 - \frac{v_2 N_2}{v_1 N_1}\right) + \frac{\chi v_2 N_2}{v}((\phi^{I})^2 - (\phi^{II})^2) = 0 \quad (3b)$$

The temperature dependence of χ is assumed to be of the form $A + B/T$, where the empirical constants correspond to the entropic (A) and enthalpic (B) contributions[33] to χ for a UCST blend.

A recognized shortcoming of the F−H equation of state is its applicability to only relatively simple, incompressible systems. Sanchez and Lacombe[30,34,35] have extended the F−H formalism to include compressible systems through the addition of free volume (empty lattice sites). The S−L equation of state has been successfully used to correlate the thermodynamic properties and phase behavior of polymer blends, as well as polymers in supercritical solutions.[2,16,30,34−37] It is given by

$$\tilde{\rho}^2 + \tilde{P} + \tilde{T}\left[\ln(1-\tilde{\rho}) + \left(1 - \frac{1}{r}\right)\tilde{\rho}\right] = 0 \quad (4)$$

where $\tilde{\rho}$, $\tilde{P}$ and $\tilde{T}$ are the reduced density, pressure, and temperature, respectively, and r represents the number

of occupied lattice sites. These reduced parameters are defined in terms of characteristic parameters, viz.,

$$\tilde{T} = \frac{T}{T^*}, \quad \tilde{P} = \frac{P}{P^*}, \quad \tilde{\rho} = \frac{\rho}{\rho^*} \tag{5}$$

where

$$T^* = \frac{\epsilon^*}{R}, \quad P^* = \frac{\epsilon^*}{v^*}, \quad \rho^* = \frac{M}{rv^*} \tag{6}$$

Here, ϵ^* is the interaction energy per repeat unit, v^* is the close-packed repeat unit volume, and M is the molecular weight. For mixtures, appropriate mixing rules must be applied. In the case of the repeat unit volume, v^* can be expressed as

$$v^* = \sum \phi_i^{\circ} v_i^* \tag{7}$$

where

$$\phi_i^{\circ} = \frac{r_i^{\circ} N_i}{rN} = \frac{\dfrac{w_i}{\rho_i^* v_i^*}}{\displaystyle\sum_j \frac{w_j}{\rho_j^* v_j^*}} \tag{8}$$

and w_i is the mass fraction of component i, and r_i° is the number of lattice sites occupied by i in the pure state. The characteristic pressure is assumed to be pairwise additive so that

$$P^* = \sum\sum \phi_i \phi_j P_{ij}^* \tag{9}$$

where

$$\phi_i = \frac{r_i N_i}{rN} = \frac{\dfrac{w_i}{\rho_i^*}}{\displaystyle\sum_j \frac{w_j}{\rho_j^*}} \tag{10}$$

and

$$P_{ij}^* = (P_i^* P_j^*)^{1/2}(1 - \delta_{ij}) \tag{11}$$

Here, δ_{ij} is a binary interaction parameter that is empirically adjusted to fit experimental data to account for system nonideality. The characteristic temperature for mixtures is given by

$$\frac{T^*}{T} = \frac{(\phi_i/\tilde{T}_i + (v_i/v_j)\phi_j/\tilde{T}_j)}{\phi_i + (v_i/v_j)\phi_j} - \frac{\phi_i \phi_j (P_i^* + P_j^* - 2P_{ij}^*)v^*}{RT} \tag{12}$$

and the corresponding chemical potential is[38]

$$\frac{\mu_i}{RT} = \ln \phi_i + \left(1 - \frac{r_i}{r}\right) + r_i\tilde{\rho}\left(\sum_{j=1}^{k} \phi_j \chi_{ij} - \sum_{i<j}^{k}\sum^{k} \phi_i \phi_j \chi_{ij}\right) + r_i\left\{-\frac{\tilde{\rho}}{\tilde{T}_i} + \frac{\tilde{P}_i\tilde{v}}{\tilde{T}} + (\tilde{v} - 1)\ln(1 - \tilde{\rho}) + \frac{1}{r_1}\ln\tilde{\rho}\right\} \tag{13}$$

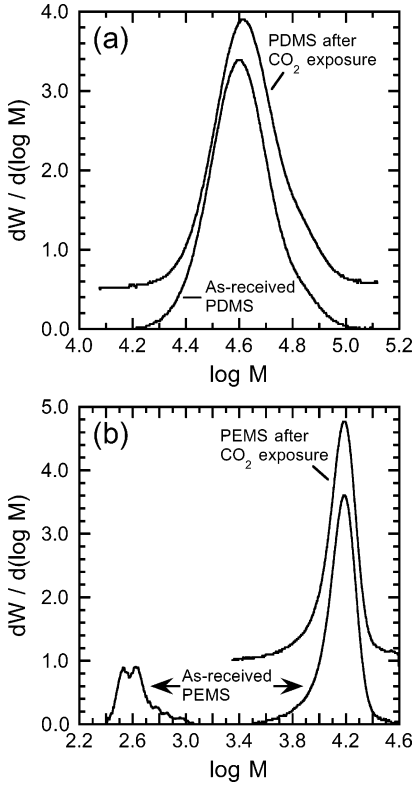

Figure 1. GPC traces acquired from (a) PDMS and (b) PEMS before and after pretreatment in high-pressure CO_2 at ~100 °C and ~34 MPa for 24 h. While the PDMS is virtually unaltered, the molecular weight distribution of PEMS is affected by exposure to CO_2, as demonstrated by the pertinent signals shown in part b. In this case, the polydispersity of the high-molecular-weight fraction decreases and a low-molecular-weight fraction, enlarged for the sake of identification in (b), disappears altogether, indicating that this fraction is dissolved in and removed by the CO_2. For this reason, all the PDMS/PEMS blends examined here are exposed to this same CO_2 pretreatment prior to analysis.

which simplifies to the following for a binary $i-j$ system:

$$\frac{\mu_i}{RT} = \ln \phi_i + \left(1 - \frac{r_i}{r_j}\right)\phi_j + r_i^{0}\tilde{\rho}\frac{(P_i^* + P_j^* - 2P_{ij}^*)v_i^*\phi_j}{RT} + r_i^{0}\left\{-\frac{\tilde{\rho}}{\tilde{T}_i} + \frac{\tilde{P}_i\tilde{v}}{\tilde{T}_i} + \tilde{v}\left[(1 - \tilde{\rho})\ln(1 - \tilde{\rho}) + \frac{\tilde{\rho}}{r_i^{\circ}}\ln\tilde{\rho}\right]\right\} \tag{14}$$

Experimental Section

Materials. The poly(dimethylsiloxane) (PDMS) ($\bar{M}_w$= 44500, $\bar{M}_w/\bar{M}_n$= 1.09) and poly(ethylmethylsiloxane) (PEMS) ($\bar{M}_w$= 14600, $\bar{M}_w/\bar{M}_n$= 1.13) homopolymers were purchased from Polymer Source (Dorval, Quebec, Canada) and individually pretreated in high-pressure CO_2 (~100 °C, ~34 MPa) for 24 h to remove any low-molecular-weight (i.e., CO_2-soluble) fraction. The molecular weight characteristics listed above correspond to the materials after pretreatment. Carbon dioxide (99.8% pure) and helium (He, >99.9% pure) were obtained from National Specialty Gases (Durham, NC). Reagent-grade toluene (Sigma-Aldrich, St. Louis, MO) was used for cleaning the sample holder and high-pressure equipment between runs.

Methods. The molecular weight distributions of the PDMS and PEMS were measured by gel permeation chromatography (GPC) at ambient temperature before and after CO_2 pretreatment. According to Figure 1a, the PDMS polydispersity (1.09) did not change noticeably upon CO_2 pretreatment, confirming the absence of a CO_2-soluble fraction. The measured molecular weight was, however, found to be significantly higher than that reported by the manufacturer (44500 vs 29000). The PEMS

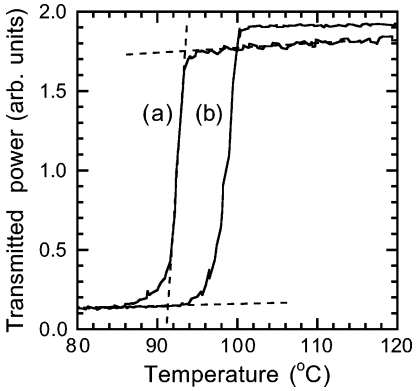

Figure 2. Representative data obtained from a 35/65 PDMS/PEMS blend in CO_2 at (a) 3.86 and (b) 6.52 MPa by high-pressure spectrophotometry, conducted at cooling rates of 3.5 and 3.9 °C/min, respectively. The inflection point of each curve, illustrated as the midpoint of the dashed line that intersects the upper and lower transmitted power limits, identifies the corresponding cloud point (T_{cp}) reported here.

polydispersity, on the other hand, was noticeably affected by CO_2 pretreatment (see Figure 1b). The polydispersity of the large peak in Figure 1b decreased from 1.16 to 1.13, and the small peak at low molecular weight (exaggerated in the figure for illustrative purposes) disappeared altogether after CO_2 pretreatment, indicating that the CO_2 extracted a small fraction of the PEMS sample. For this reason, all blend constituents were pretreated according to the same procedure before cloud point temperatures were measured. To ascertain the extent to which long-term exposure to high-pressure CO_2 affected blend characteristics, specimen mass loss incurred during pretreatment was measured gravimetrically and found to be less than ~1%, which corresponds to a maximum change in composition of only ±2.5%. Attempts to measure blend compositions by liquid-state ^{29}Si and ^{1}H NMR yielded changes that were less than or equal to that determined by gravimetric analysis.

The cloud point temperature (T_{cp}) of each PDMS/PEMS blend examined here was determined as a function of CO_2 pressure by high-pressure spectrophotometry. Each blend was placed in a clear quartz tube with a flat bottom, and the tube was then placed in a high-pressure cell with sapphire windows. The initially homogeneous specimen was slowly cooled at ~1−4 °C/min (with no substantial variation in results) from the single-phase region at constant CO_2 pressure (ranging from 0 to ~35 MPa), and the change in turbidity was monitored with a 632 nm laser source oriented vertically relative to a photometric power meter. Visual inspection verified that recorded turbidity changes identified phase separation of the blend and not CO_2 bubble formation. Pressure, temperature, and transmitted beam power measurements were computer-interfaced and measured as a function of time. Figure 2 displays two examples of the transmitted laser power vs temperature curves generated in this manner. The T_{cp} values reported herein correspond to the temperature at the inflection point of each curve. Phase separation typically occurred over a temperature range of 5−10 °C. After each pressure jump, the system was held in the single-phase region for at least 4 h to allow equilibration with CO_2 before measuring T_{cp}. A similar procedure was followed for complementary tests using He instead of CO_2. While the blend (24 wt % PDMS) was pretreated with CO_2 to ensure comparable blend characteristics, the equilibration period was reduced (to ~45 min) to limit dissolution of He into the molten blend.

Results and Discussion

Measured cloud point temperatures are presented as a function of CO_2 pressure in the vapor phase (hereafter referred to simply as pressure) in Figure 3 for the various blend compositions examined in this work. In

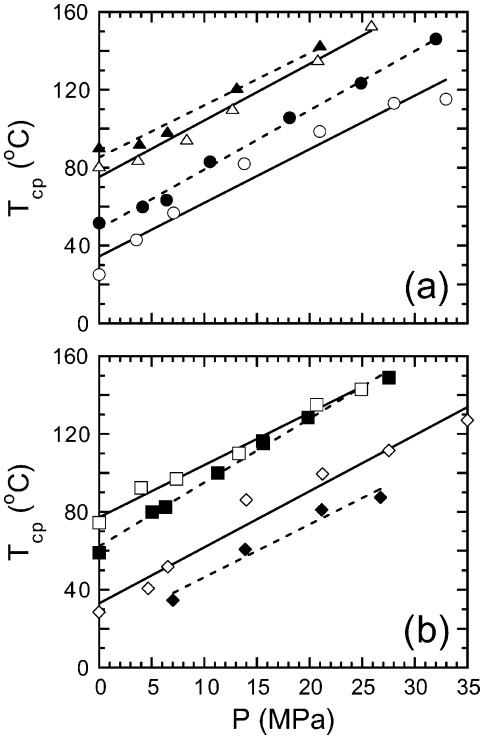

Figure 3. Dependence of the PDMS/PEMS cloud point temperature (T_{cp}) on CO_2 pressure in the vapor phase for a series of blends that are rich in (a) PEMS and (b) PDMS. The compositions of these blends (in wt % PDMS solvent-free) are as follows: 6 (○), 10 (●), 20 (△), 35 (▲), 51 (□), 62 (■), 80 (◇) and 90 (◆). The solid and dashed lines constitute linear regressions to the data. These results indicate that the presence of CO_2 generally promotes PDMS/PEMS immiscibility by shifting each T_{cp} to higher temperatures with increasing pressure.

the absence of CO_2, T_{cp} increases as w_{PDMS} is increased up to about 25 wt % and then decreases, revealing that (i) the critical composition lies near 25 wt % PDMS, (ii) the critical temperature is ~91 °C, and hence, (iii) the coexistence curve appears asymmetric with regard to composition. Such asymmetry is a consequence of the difference in molecular weights between the PDMS and PEMS used here. Another feature evident from the data in this figure is that T_{cp} increases monotonically with increasing pressure over the range of pressure investigated (up to ~35 MPa). Close observation reveals that this dependence of T_{cp} on pressure is nearly linear, independent of polymer blend composition. Such functional similarity strongly suggests that a master curve can be generated. Figure 4 shows the variation of ΔT_{cp}, defined as $T_{cp}(P) - T_{cp}(\text{no } CO_2)$, with pressure and confirms that all the data portrayed in Figure 3 effectively shift onto a single line with a slope of 2.9 ± 0.3 °C/MPa. Thus, the data provided in these two figures confirm that high-pressure CO_2 serves to reduce the miscibility of PDMS/PEMS blends by shifting the two-phase envelope to higher temperatures. This behavior is in contrast to the previous finding of Beiner et al.[20] that application of hydrostatic pressure enhances the miscibility of PDMS/PEMS blends.

As mentioned earlier, the reported[20] reduction in T_{cp} with increasing hydrostatic pressure in PDMS/PEMS blends is attributed to the negative ΔV_{mix}. According to the data shown in Figures 3 and 4, however, use of (CO_2) pressure, rather than hydrostatic pressure, yields a pronounced increase in T_{cp} with increasing pressure, in which case ΔV_{mix} would be positive according to (ΔUCST/

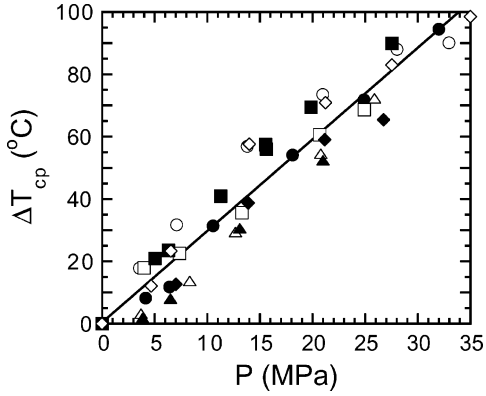

Figure 4. Master curve of ΔT_{cp}, defined as $T_{cp}(P) - T_{cp}(\text{no } CO_2)$ and presented as a function of CO_2 pressure in the vapor phase, confirming that all the data displayed in Figure 3 shift onto a single (solid) line with a slope of ~2.9 °C/MPa. The symbols are the same as those used in Figure 3.

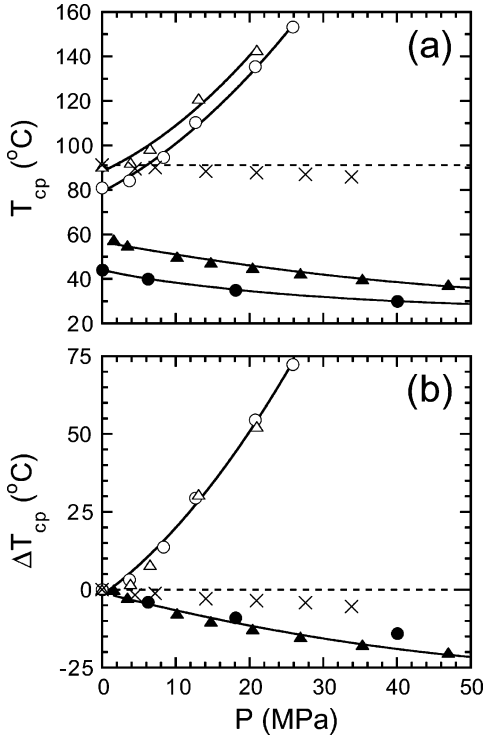

Figure 5. Variation of (a) T_{cp} and (b) ΔT_{cp} with pressure from different sources for several PDMS/PEMS blends. Two blends prepared from the present homopolymers with compositions of 20 (○) and 35 (△) wt % PDMS are exposed to high-pressure CO_2, whereas one with 24 wt % PDMS (×) is subjected to high-pressure He. The responses of two blends described by Beiner et al.[20] with compositions of 47 (●) and 51 (▲) wt % PDMS to hydrostatic pressure are included. The solid lines serve as guides for the eye, and the horizontal dashed line corresponds to the neat cloud point for the 24/76 PDMS/PEMS blend in part a and the condition of $\Delta T_{cp} = 0$ in part b.

$\Delta P)_\phi = (T\Delta V_{mix}/\Delta H_{mix})$. Cloud point measurements illustrating this difference are displayed for comparison in Figure 5a and clearly illustrate that, by swelling the polymer melt (even in the presence of hydrostatic pressure) and screening intermolecular interactions, CO_2 has a profound impact on ΔV_{mix}. To simulate the effects of hydrostatic pressure on our system, we have examined the phase behavior of a single PDMS/PEMS blend with 24 wt % PDMS (near the critical composition) in the presence of high-pressure He, which is much less soluble than CO_2 (by at least 2 orders of magnitude[17])

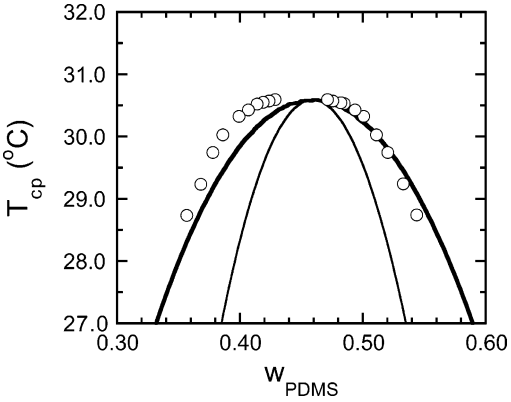

Figure 6. Comparison of the phase-equilibrium data reported by Kuwahara et al.[18] and the regressed F−H equation of state used to extract $\chi(T)$. The thick line represents the predicted coexistence (binodal) curve, whereas the thin line denotes the corresponding stability (spinodal) curve.

in either PDMS or PEMS. Since He does not swell either polymer to an appreciable extent and since there are fewer dissolved He molecules available to screen intermolecular interactions, it follows that the effect of high-pressure He on ΔT_{cp} should be closer, but not identical (due to nonzero solubility), to that achieved by hydrostatic pressure alone. This expectation is confirmed in Figure 5b, wherein $\Delta T_{cp}/\Delta P_{He} \approx -0.14$ °C/MPa.

Binary Systems: PDMS/PEMS Blends. In the F−H model, the temperature dependence of χ (expressed in terms of $A + B/T$) is required to predict the phase behavior of the PDMS/PEMS blends in the absence of CO_2. Unfortunately, values of A and B reported in the literature for this system vary somewhat, as can be seen in Table 1. Included in this table are values of A and B that we obtained by fitting the F−H equation of state to the coexistence data of Kuwahara et al.[18] (due to its precision and high quality). The regressed binodal curve is compared with the experimental data of Kuwahara et al.[18] in Figure 6 and shows reasonably good agreement. Included in Figure 6 is the predicted spinodal curve for the sake of completeness. Phase diagrams computed with the various A and B values listed in Table 1 are compared with experimental data acquired from the present PDMS/PEMS blends in the absence of CO_2 (Figure 7a) and demonstrate that the predicted coexistence curve based on our regressed parameters most closely matches our experimental data. Differences in the values of A and B from various sources could be related to measurement accuracy, analytical method, and/or sample quality. Further investigation beyond the scope of this work is necessary to determine the source of such variability, as well as the reason why predictions derived from the data of Kuwahara et al.[18] most closely match our experimental data. Corresponding values of χ are displayed as a function of reciprocal temperature in Figure 7b and confirm that our A and B parameters yield results that are consistent with data previously reported[22,24] for this system.

Ternary Systems: PDMS/PEMS Blends in the Presence of CO_2. One-, two- and three-phase regions can exist simultaneously in ternary systems under the right set of temperature−pressure conditions, and the shapes of such regions may differ markedly from system to system or over a range of conditions.[39] In the present work, we are concerned exclusively with the conditions responsible for vapor−liquid−liquid equilibria (VLLE) in the PDMS/PEMS/CO_2 system. More specifically, we

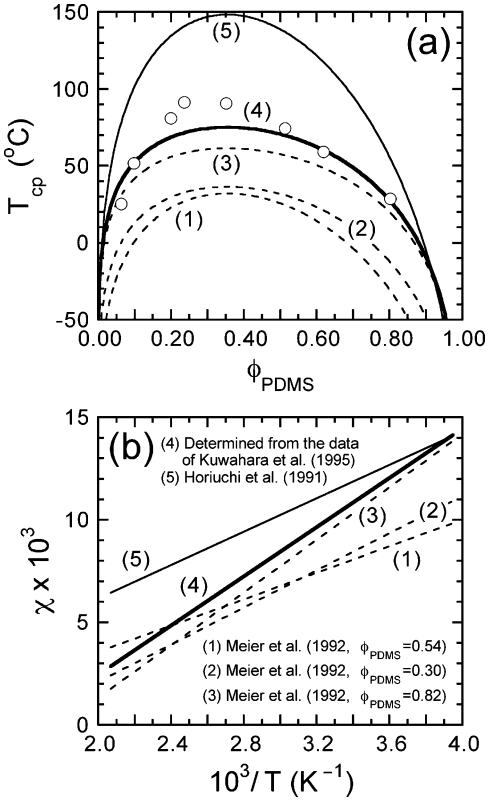

Figure 7. Comparison of the experimental PDMS/PEMS phase diagram generated in this work in the absence of CO_2 (a) with predictions derived from the F−H equation of state using several different $\chi(T)$ expressions[18,22,24] of the form $\chi = A + B/T$ (b) and molecular weights identical to those of the polymers examined in this study. The numerical designations and line types used in part a identify the corresponding $\chi(T)$ relationships displayed in part b. The $\chi(T)$ relation derived from Figure 6 (thick line) provides the best quantitative agreement with the present data.

seek to use the S−L equation of state to elucidate the effect of pressure on the temperatures corresponding to the cloud points of PDMS/PEMS polymer blends. The first step in the application of an equation of state to multicomponent mixtures is to determine the pure-component parameters. Within the S−L framework, the pure component parameters (P^*, T^*, and ρ^*) are normally regressed from experimental vapor pressure and liquid density data. While this procedure is straightforward for small molecules (e.g., CO_2), pure-component parameters for polymers are generally determined from liquid volumetric data[2,35] since (i) high-molecular-weight polymers have no detectable vapor pressure and (ii) they thermally degrade before exhibiting a critical point. The S−L parameters for CO_2 and PDMS used in this work have been obtained by these procedures.[30] However, corresponding parameters for PEMS have not, to the best of our knowledge, been reported for the S−L (or, in fact, any) equation of state. The absence of such information may reflect the sparse amount of experimental data currently available for this polymer.

Liquid volumetric data are available for a single PEMS homopolymer with a molecular weight of 31200 by Enders et al.,[19] who provide a linear regression for the density of PEMS over the temperature range 20 to 100 °C. Since the PDMS densities also obtained by Enders et al.[19] are systematically higher than other reported data and their PEMS density correlation represents the only available experimental data for this homopolymer, we have elected to shift their PDMS data by ∼1% to achieve consistency with the literature. Since the same pycnometer was used in both sets of measurements, we assume that the same shift applies to their PEMS correlation, which results in a corrected density correlation: $\rho_{PEMS} = 0.976 - 5.4 \times 10^{-4}T$, where T in this one instance is given in °C. We further assume that the pressure dependence of PEMS is similar to that of PDMS due to the similarity of their chemical structures. Although these assumptions are ad hoc, it will be shown that the S−L parameters obtained in this fashion yield predictions that are in reasonably good agreement with the experimental data presented in this work. When experimental data for PEMS become more readily available, the analysis presented here could be reexamined. Table 2 summarizes the pure-component S−L parameters used throughout the remainder of this work. From a careful analysis of binary and ternary blends of low-polydispersity blends, Horiuchi et al.[22] conclude that the PDMS/PEMS pair exhibits no evidence of specific interactions, in which case $\delta_{PDMS/PEMS}$ can be set equal to zero. Moreover, we assume $\delta_{PEMS/CO_2} = \delta_{PDMS/CO_2} = -0.218 + 9.67667 \times 10^{-3}T - 9.05 \times 10^{-5}T^2 + 2.83 \times 10^{-7}T^3$, which is obtained from PDMS/CO_2 experimental data.[37]

Table 2. Characteristic Sanchez−Lacombe Equation of State Parameters Used in This Study

species	P^* (MPa)	T^* (K)	ρ^* (kg/m^3)	ref
CO_2	464.2	328.1	1426	30
PDMS	302.0	476.0	1104	30
PEMS	302.0	552.0	1126	this work

Once the S−L parameters are known, standard thermodynamic relations are employed to solve for the conditions of phase equilibrium on the basis of equality of temperature, pressure and chemical potential of each component in all phases. These conditions are determined here using a minimization numerical algorithm.[40] It is important to mention that the vapor phase was presumed to be pure CO_2. Although presenting the results of our calculations in the form of ternary diagrams could provide more information (e.g., the composition of CO_2 in the liquid phases), we prefer to display our results on a solvent-free basis to facilitate comparison with the experimental data. Coexistence curves computed from the S−L equation of state are shown as a function of blend composition (on a solvent-free basis) in Figure 8 and are observed to be in good quantitative agreement with the experimental data up to 20 MPa. Polymer−polymer cloud point curves predicted from the S−L formalism for the 30 MPa isobar are included in Figure 8. Other thermodynamic properties of interest can be extracted from the above analysis. The binary interaction parameter (χ), for instance, is directly related to the change in chemical potential of a component upon mixing. Compilations of χ are available for solvent−polymer solutions[41] and polymer blends.[32] Whereas the polymer−solvent interaction parameters ($\chi_{PDMS-CO_2}$ and $\chi_{PEMS-CO_2}$) were also calculated here, we only consider further the polymer−polymer interaction parameter ($\chi_{PDMS-PEMS}$, hereafter referred to simply as χ) as an explicit function of pressure.

The Flory−Huggins theory[31] predicts that, at constant volume, the difference between the residual chemical potential per segment of component 1 (μ_i) and the residual chemical potential per segment of pure 1 (μ_i^0) in a symmetric binary polymer blend is related to

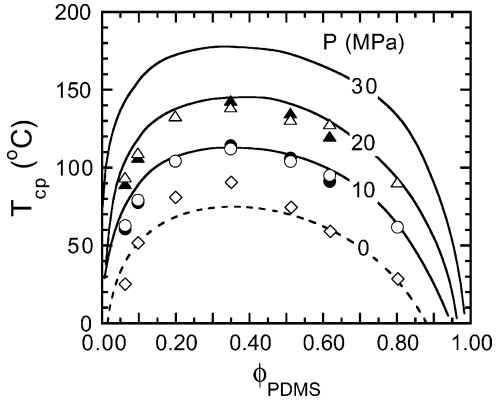

Figure 8. Measured and predicted PDMS/PEMS phase diagrams at different pressures (labeled). Experimental data collected in the absence of CO_2 are identified (◇), and interpolations of the data at 10 and 20 MPa determined from the master curve displayed in Figure 4 (open symbols) and the composition-specific data shown in Figure 3 (filled symbols) are represented by circles and triangles, respectively. The dashed line signifies predictions from the F−H equation of state (equivalent to curve 4 in Figure 7a), whereas solid lines denote predictions from the S−L equation of state.

composition by

$$\frac{(\mu_i - \mu_i^0)^{res}}{RT} = \chi^{eff}\phi_i^2 \qquad (15)$$

A similar expression can be applied to solvent−polymer−polymer solutions where the solvent is component 1. In this fashion, an effective χ parameter can be ascertained from the S−L equation of state as a function of composition, temperature and pressure. Determination of interaction parameters in a ternary system is very complex, because they can depend not only on temperature, but also on pressure and composition. In some cases, it can be expected that the influence of some of these variables is relatively negligible. Several independent studies[19,22,23] of PDMS/PEMS blends have, for example, shown that χ is independent of blend composition. An exception to these findings is the work of Meier et al.,[24] who provide evidence for the composition dependence of χ. The results presented in the previous section, however, indicate that a single $\chi(T)$ function adequately fits our data without requiring a composition-dependent χ.

While interaction parameters between the solvent and each polymer can, on the other hand, be expected to be composition-dependent, we assume that the effect of CO_2 is comparable for PDMS and PEMS due to their structural similarity. Values of χ extracted from the S−L equation of state are shown as a function of reciprocal temperature in Figure 9a for several pressures. In the absence of CO_2, χ varies linearly as $A + B/T$, with the values of A (=−0.0104) and B (=7.26) being slightly higher than those determined from the F−H analysis discussed earlier (see Table 1). Although the origin of this marginal difference has not been explored in this study, we suspect that it may reflect some of the assumptions made regarding PEMS. As CO_2 is introduced into the PDMS/PEMS blend, χ is found to increase systematically. In fact, a linear $\chi(T)$ relationship is retained at each of the pressures examined, in which case χ can be expressed in the general form $A(P) + B(P)/T$. Values of A and B are displayed as functions of pressure in Figure 9b and reveal that A increases (or

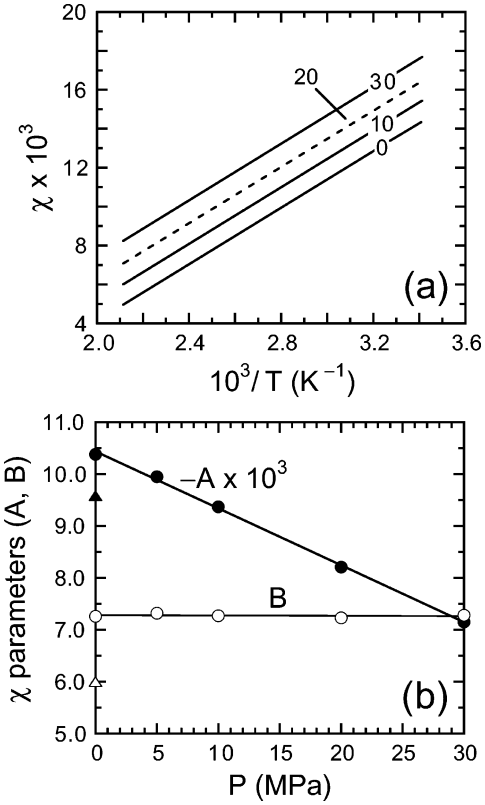

Figure 9. (a) Temperature dependence of χ provided as a function of pressure (labeled, in MPa) from predicted phase diagrams such as those displayed in Figure 8. (b) Pressure-dependent values of the χ parameters A (●) and B (○) predicted from the S−L equation of state for the generic expression of χ (=$A + B/T$). Values of A and B deduced from the F−H equation of state are included (▲ and △, respectively) for comparison. The solid lines denote linear regressions to the predicted A and B parameters.

$-A$ decreases) linearly with increasing pressure, whereas B appears to be independent of pressure. The physical implication of this intriguing result is currently the focus of a complementary study[42] that employs the statistical associating fluid theory in an effort to elucidate the general thermodynamic behavior of polymer blends in the presence of high-pressure CO_2.

Conclusions

Exposure of polymer blends to highly compressible, supercritical fluids provides a facile means by which to modify phase behavior, which can be exploited in the development of new processing routes or materials.[3,43] In this work, we have examined the phase-separation behavior of PDMS/PEMS blends in the presence of high-pressure CO_2. This UCST blend is unique in that it inherently exhibits a negative change in volume upon mixing, which results in enhanced miscibility (signified by a reduction in cloud point temperature) upon exposure to hydrostatic pressure.[20] We have qualitatively reproduced this result by using high-pressure He, which exhibits very low solubility in, and negligible swelling of, PDMS and PEMS. In the presence of high-pressure CO_2, however, both homopolymers swell extensively due to relatively high CO_2 uptake,[8] and their phase behavior is significantly altered: they become increasingly immiscible as the CO_2 pressure is increased. These results are found to collapse onto a master curve of $\Delta T_{cp}(P)$ for pressures up to ∼35 MPa.

To investigate the underlying thermodynamics responsible for reduced blend miscibility, we have analyzed the data of Kuwahara et al.[18] in the context of the Flory−Huggins equation of state to extract the temperature dependence of χ, which yields a predicted phase diagram that closely resembles the experimental one reported herein. The phase diagram of the ternary PDMS/PEMS/CO_2 system (expressed on a solvent-free basis) predicted with the Sanchez−Lacombe equation of state agrees well with the experimental results obtained in this work. Corresponding values of χ signifying the interaction between PDMS and PEMS are presented as functions of temperature and pressure. Further analysis of this outcome with a molecularly descriptive equation of state[42] is currently underway.

Acknowledgment. This study was supported by the Kenan Center for the Utilization of Carbon Dioxide in Manufacturing and the STC Program of the National Science Foundation under Agreement No. CHE-9876674. We thank Dr. Sarah Folk (University of North Carolina at Chapel Hill) and Dr. Hanna S. Gracz (North Carolina State University) for technical assistance with the GPC and NMR measurements, respectively.

References and Notes

(1) Bungert, B.; Sadowski, G.; Arlt, W. *Ind. Eng. Chem. Res.* **1998**, *37*, 3208.
(2) Kirby, C. F.; McHugh, M. A. *Chem. Rev.* **1999**, *99*, 565.
(3) Kazarian, S. G. *Polym. Sci. C* **2000**, *42*, 78.
(4) Cooper, A. I. *J. Mater. Chem.* **2000**, *10*, 207; *Adv. Mater.* **2001**, *13*, 1111.
(5) DeSimone, J. M. *Science* **2002**, *297*, 799.
(6) Utracki, L. A. *Polymer Alloys and Blends: Thermodynamics and Rheology*; Oxford University Press: New York, 1990.
(7) Chiou, J. S.; Barlow, J. W.; Paul, D. R. *J. Appl. Polym. Sci.* **1985**, *30*, 2633.
(8) Royer, J. R.; DeSimone, J. M.; Khan, S. A. *Macromolecules* **1999**, *32*, 8965.
(9) Zhong, Z.; Zheng, S.; Mi, Y. *Polymer* **1999**, *40*, 3829.
(10) Walker, T. A.; Melnichenko, Y.; Wignall, G. D.; Lin, J. S.; Spontak, R. J. *Macromol. Chem. Phys.* **2003**, *204*, 2064.
(11) Flichy, N. M. B.; Kazarian, S. G.; Lawrence, C. J.; Briscoe, B. J. *J. Phys. Chem. B* **2002**, *106*, 754.
(12) Royer, J. R.; Gay, Y. J.; Adam, M.; DeSimone, J. M.; Khan, S. A. *Polymer* **2002**, *43*, 2375.
(13) Walker, T. A.; Raghavan, S. R.; Royer, J. R.; Smith, S. D.; Wignall, G. D.; Melnichenko, Y.; Khan, S. A.; Spontak, R. J. *J. Phys. Chem. B* **1999**, *103*, 5472.
(14) Vogt, B. D.; Brown, G. D.; RamachandraRao, V. S.; Watkins, J. J. *Macromolecules* **1999**, *32*, 7907.
(15) Watkins, J. J.; Brown, G. D.; RamachandraRao, V. S.; Pollard, M. A.; Russell, T. P. *Macromolecules* **1999**, *32*, 7737. RamachandraRao, V. S.; Watkins, J. J. *Macromolecules* **2000**, *33*, 5143.
(16) Kazarian, S. G., Chan, K. L. A. *Macromolecules* **2004**, *37*, 579.
(17) Kuo, A. C. M. In *Polymer Data Handbook*; Mark, J. E., Ed.; Oxford University Press: Oxford, England, 1999; pp 411−435.
(18) Kuwahara, N.; Sato, H.; Kubota, K. *Phys. Rev. Lett.* **1995**, *75*, 1534.
(19) Enders, S.; Stammer, A.; Wolf, B. A. *Macromol. Chem. Phys.* **1996**, *197*, 2961.
(20) Beiner, M.; Fytas, G.; Meier, G.; Kumar, S. K. *Phys. Rev. Lett.* **1998**, *81*, 594.
(21) Beiner, M.; Fytas, G.; Meier, G.; Kumar, S. K. *J. Chem. Phys.* **2002**, *116*, 1185.
(22) Horiuchi, H.; Irie, S.; Nose, T. *Polymer* **1991**, *32*, 1970.
(23) Chopra, D.; Kontopoulou, M.; Vlassopoulos, D.; Hatzikiriakos, S. G. *Can. J. Chem. Eng.* **2002**, *80*, 1057.
(24) Meier, G.; Momper, B.; Fischer, E. W. *J. Chem. Phys.* **1992**, *97*, 5884.
(25) Theobald, W.; Meier, G. *Phys. Rev. E* **1995**, *51*, 5776. Theobald, W.; Sans-Penninckx, A.; Meier, G.; Vilgis, T. A. *Phys. Rev. E* **1997**, *55*, 5723.
(26) Sato, H.; Kuwahara, N.; Kubota, K. *Phys. Rev. E* **1996**, *53*, 3854.
(27) Melnichenko, Y. B.; Wignall, G. D.; Schwahn, D. *Phys. Rev. E* **2002**, *65*, 061802.
(28) Meier, G.; Fytas, G.; Momper, B.; Fleischer, G. *Macromolecules* **1993**, *26*, 5310.
(29) Walsh, D. J.; Rostami, S. *Macromolecules* **1985**, *18*, 216.
(30) Sanchez, I. C.; Lacombe, R. H. *Macromolecules* **1978**, *11*, 1145.
(31) Flory, P. J. *J. Chem. Phys.* **1941**, *9*, 660. Flory, P. J. *Principles of Polymer Chemistry*; Cornell University Press: Ithaca, NY, 1953. Huggins, M. L. *J. Phys. Chem.* **1941**, *9*, 440.
(32) Balsara, N. P. In *Physical Properties of Polymers Handbook*; Mark, J. E., Ed.; AIP Press: Woodbury, NY, 1996; Chapter 19.
(33) Bates, F. S. *Science* **1991**, *251*, 898.
(34) Lacombe, R. H.; Sanchez, I. C. *J. Phys. Chem.* **1976**, *80*, 2558.
(35) Sanchez, I. C.; Lacombe, R. H. *J. Phys. Chem.* **1976**, *80*, 2352.
(36) Kiszka, M. B.; Meilchem, M. A.; McHugh, M. A. *J. Appl. Polym. Sci.* **1988**, *36*, 583.
(37) Garg, A.; Gulari, E.; Manke, W. *Macromolecules* **1994**, *27*, 5643.
(38) Sanchez, I. C.; Panayiotou, C. G. In *Models for Thermodynamic and Phase Equilibria Calculations*; Sandler, S. I., Ed.; Marcel Dekker: New York, 1994.
(39) Wallas, S. M. *Phase Equilibria in Chemical Engineering*; Butterworth: Stoneham, MD, 1985.
(40) Press, W. H.; Teukolsky, S. A.; Vetterlin, W. T.; Flannery, B. P. *Numerical Recipes in Fortran*; Cambridge University Press: Cambridge, England, 1986.
(41) Orwoll, R. A.; Arnold, P. A. In *Physical Properties of Polymers Handbook*; Mark, J. E., Ed.; AIP Press: Woodbury, NY, 1996; Chapter 14.
(42) Colina, C. M.; Walker, T. A.; Spontak, R. J.; Gubbins, K. E. Manuscript in preparation.
(43) Walker, T. A. Ph.D. Dissertation, North Carolina State University, 2003.

MA034920O